STEADY-STATE HEAT TRANSFER TO BOILING LIQUID HELIUM IN SIMULATED COIL WINDINGS*

P. L. Walstrom

Oak Ridge National Laboratory
Bldg. 9204-1/MS-14, P.O. Box Y
Oak Ridge, Tennessee 37830

INTRODUCTION

Three of the six superconducting toroidal field magnets being built for testing in the Large Coil Test Facility at Oak Ridge National Laboratory are to be cooled by pool boiling in liquid helium at 4.2 K; these include two U.S. coils, made by General Electric (GE) and General Dynamics (GD), and the Japanese coil. All three coils are designed to be cryostable. In the present investigation, a test bundle simulating the GE/LCT winding pack, instrumented with heaters and thermocouples, was tested to determine its steady-state heat transfer behavior. The results indicate that with the as-wound conductor the GE/LCT magnet will recover only by cold-end conduction in small regions where the conductor is nearly horizontal.

Test Bundle Configuration and Test Procedures

The GE/LCT conducting element is formed by cabling sixteen 3.4-mm-square cross-section subelements around a rounded rectangular 3.5- by 35-mm cross-section copper core, soldering in a bath, and squaring in a Turk's head die to final dimensions of 42 by 10 mm. The subelements are made by inserting a squared NbTi multifilamentary composite wire into a U-shaped copper carrier. The subelements, separated by 1.8-mm-wide gaps and angled at 20°

*Research sponsored by the Office of Fusion Energy, U.S. Department of Energy, under contract W-7405-eng-26 with the Union Carbide Corporation.

from the conductor axis, form a pattern of parallel channels approximately 12 cm long.

The conductor is pancake wound with the wide face down. Turn-to-turn insulation is provided by a 42-mm-wide by 0.25-mm-thick strip of Nomex* paper insulation. Pancake-to-pancake insulation is provided by grooved, unperforated epoxy-fiberglass sheets. The three winding pack constituents are shown in Fig. 1. The test bundle (Fig. 2) is a stack 12 pieces high of 30.5-cm lengths of GE/LCT-coil 8-T grade conductors separated by the Nomex paper strips. Heaters were installed in three of the conductor pieces by pulling the superconducting multifilamentary composite wire from the surrounding copper carriers and soldering stainless-steel-sheathed, MgO-insulated Nichrome wires into the resultant grooves. The stack was divided into three groups of four conductor pieces, the heated piece being the second one from the bottom in each group of four pieces. The conductors in the lower two groups were modified by drilling 1-mm-diam holes (with an average of two per groove) between subelements and through the core, where grooves on the top side coincided with grooves on the bottom side. Eight Au-0.07 at. % Fe vs copper thermocouples with reference junctions in the bath were installed in each of the three heated conductor pieces (four in the subelements and four in the core between subelements). The unheated pieces immediately above and below the heated pieces were each instrumented with two thermocouples in the core.

In assembling the stack Nomex strips, modified by punching them with 4-mm-diam holes on 0.5-in. centers in a rectangular pattern with six holes per inch length of conductor, were placed between the conductor pieces in the lowermost group of four pieces. Unperforated Nomex strips were placed between pieces of the other two groups. The stack of 12 instrumented pieces was placed between two grooved pieces of G-10 epoxy-fiberglass insulating sheets with the same groove and land dimensions as the GE/LCP interpancake spacers. The stack with surrounding insulation was placed in a clamping mechanism (Fig. 2), and the aluminum bolts tightened for an estimated pressure of about 14 MPa (2000 psi) after cooldown, a typical value for the GE/LCT coil windings when energized. The clamping mechanism and the stack were placed in a pivot mechanism with an activating rod extending to room temperature which allowed continuous variation of angle from -3° to 90° from horizontal when the sample was in a liquid helium bath.

---

*Reference to a company or product name does not imply approval or recommendation of the product by Union Carbide Corporation or the U.S. Department of Energy to the exclusion of others that may be suitable.

Fig. 1. GE/LCT coil winding pack elements.

The measurement system is shown schematically in Fig. 3. The heater current is supplied by a 50-V, 20-A operational power supply programmed to produce 39 equal power steps for a staircase-up, staircase-down time dependence. The heater power was held constant for 5 s at each power level. The heater current was measured by a resistive shunt. The heater voltage signal, attenuated by a 10:1 resistive divider, and the current shunt signal were isolated by differential amplifiers. The amplifier outputs were fed into the high level input channels of an Analogic computer-controlled scanner/digitizer which was interfaced to a PDP-11/03 microcomputer with a 64-K word memory. The 12 thermocouple signals from a heated conductor piece and the adjacent unheated pieces were input directly to the low level input channels of the Analogic scanner. The Analogic scanner was programmed to sample each of the voltage, current, and 12 thermocouple signals 25 times per second. The raw data were buffered and written out onto a floppy disk by the PDP-11/03 system. The contents of the floppy disk were read, converted to physical units, and plotted by a PDP-11/60 system equipped with a printer/plotter.

Test Results and Discussion

Figure 4 is a computer-generated plot of data from the sample with unmodified conductor and insulation at 0° showing the temperature traces derived from four thermocouple signals by use of the

Fig. 2. Assembled test bundle in pivot mechanism.

NBS tables. The data were smoothed by averaging ten points at a time. The traces for the end of the sample are consistently lower than the traces for the middle, as would be expected as a result of the fact that the channels are shorter at the ends. The subelement temperature at the center of the sample is consistently greater than the core temperature. An elementary calculation shows that even if all of the heater power flux was conducted through the subelement to the core without heat transfer to the liquid from the subelement, the temperature drop through the height of the subelement could only be a few hundredths of a degree; the much larger observed temperature difference must be due to incomplete solder bonding of the subelement to the core. The latter conclusion is borne out by destructive examination of production specimens. The constituents of the sample, however, are sufficiently well coupled thermally to exhibit breakaway

Fig. 3. Signal conditioning, data acquisition, and control system block diagram.

(defined here as an abrupt change in slope at the lower end of the film boiling portion of the heat transfer curve) at the same power level; therefore, the breakaway flux data can be applied without large errors to the magnet itself, in which heat is generated both in the core and in the subelements in the event a normal zone is formed in the conductor. (The above deficiency, of course, could have been eliminated by installing heaters in the core, somehow, but this was not feasible with production conductor specimens.)

The temperature traces in Fig. 4 exhibit, in addition to hysteresis (i.e., different temperatures for increasing and decreasing power levels at the same flux), transient behavior on a long time scale. At nucleate boiling flux levels the sample reaches fairly stable temperatures (fluctuations of less than ±0.05 K) in less than a second; at the higher power levels, stable temperatures are not reached in 5 s in some cases. The time scale for this behavior must be related to times required to set up stable, thermally driven two-phase flow patterns because relevant conduction time constants in solid constituents are an order of magnitude less.

Figures 5, 6, and 7 are plots of the heat flux vs the stabilized temperature rise measured for subelements at the middle of the heated samples at various angles of the conductor axis from horizontal. Two scales on the ordinate are shown: the usual power/wetted area scale, with an assumed wetted perimeter of 13.8 cm, and power per unit cell volume, where the unit cell, a

Fig. 4. Computer-generated plot of temperature vs time for four locations on the unmodified specimen at 0°.

rectangular parallel pipe, has here a height equal to the conductor height plus the thickness of the turn-to-turn insulation and a width equal to the conductor width plus the thickness of the interpancake insulation. The latter scale is useful in comparing the effectiveness of different conductor/cooling channel designs based on steady-state heat transfer because it does not depend on inherently arbitrary definitions of wetted perimeter and because it exhibits the tradeoff between wetted perimeter and heat transfer degradation due to channel restrictions. Significant hysteresis is observed only for the unmodified (top) heated sample at 0° and for the middle (holes in core but not in Nomex) sample at 0° and -3°. (Data were taken at -3° as a check on the angular accuracy of the pivot mechanism near 0°.) Comparisons of the 0° curves in Figs. 5, 6, and 7 show that addition of the holes to the core alone improves the 0° heat transfer only slightly, while the addition of holes to the turn-to-turn insulation, which allows

Fig. 5. Curves of steady-state heating power density vs temperature rise above the bath temperature for the unmodified conductor sample at various angles from horizontal.

vertical flow, increases the breakaway flux significantly — about 35%. The latter modification to the GE/LCT coil design was not made because of concern about turn-to-turn shorts; such a modification would be feasible if a thicker turn-to-turn insulation were to be used. Temperature traces for the unheated conductor pieces above and below the heated sample show insignificant temperature rise at breakaway flux power levels for the top and middle samples (no holes in turn-to-turn insulation) and a small rise (0.2 K) for the unheated sample above the heated sample with intervening perforated turn-to-turn insulation. This would not be sufficient to drive the analogous adjacent turn normal in the magnet, for which the current-sharing threshold temperature difference from the bath temperature is 0.8 K or more.

For the unmodified (no holes) specimen only (Fig. 5), an interesting temperature oscillation phenomenon was observed at 5° and 10°. These data points are designated by double-ended arrows

Fig. 6. Curves of steady-state heating power density vs temperature rise above the bath temperature for a conductor sample with holes drilled in the core but with unperforated turn-to-turn insulation.

between the two temperature extremes reached; the period of the oscillation was approximately 1 s.

In an attempt to determine the effect of the grooved G-10 interpancake insulation on the steady-state heat transfer, an additional set of curves was obtained for which the interpancake insulation and side clamping plates were removed, allowing unrestricted flow from the channels between the subelements to the bath. For comparison, data for two angles (0° and 20°) of the top (no holes) sample are shown in Fig. 8 along with the data for the same sample with the interpancake insulation in place. Only a very slight improvement in heat transfer is observed for the 0° data after removal of the interpancake insulation, but the 20° curve with the interpancake insulation removed lies considerably above the curve from the data for which the insulation was in place. Behavior similar to the 20° curve was observed for the other angles away from horizontal. The data demonstrate the limiting effect on the heat transfer of the long horizontal heated channels.

Fig. 7. Curves of steady-state heating power density vs temperature rise above the bath temperature for a conductor sample with holes drilled in the core and with perforated turn-to-turn insulation.

Table I is a comparison of the data from the present test with data from similar tests performed on test bundles simulating the windings of the other pool-boiling LCT coils.[1,2] Also shown for comparison are data from a previously reported steady-state heat transfer experiment for a similar conductor[3] with channels of approximately the same length (13 cm) but with more area than the GE/LCT coil (3.1 x 3.1 mm vs 3.4 x 1.8 mm). The Japanese coil data are considerably higher than the two U.S. coils, even when power/unit cell volume, a fairer basis of comparison, rather than power/unit area is used. The high breakaway flux obtained for the Japanese winding design can be attributed to the coated, highly developed surface and the large (8 cm x 2.9 mm) cooling channels between the pancakes. The GD/LCT coil designers also tested the effects of modifying their conductor with a chemical treatment (Ebanol C) and observed a 40% increase in heat transfer, but they did not use it for reasons of cost.

Fig. 8. Comparison of steady-state heat transfer data for an unmodified sample at 0° and 20° from horizontal with and without interpancake insulation.

CONCLUSIONS

The present data show that the worst case steady-state stability in the GE/LCT magnet windings is at a horizontal conductor orientation. The heat transfer improves with inclination of the conductor from horizontal. Calculations[4] show that for these small regions normal zones will recover by cold-end conduction from the inclined conductor on either end.

ACKNOWLEDGMENTS

The author is indebted to P. F. Michaelson and C. L. Linkenhoker of the General Electric Co. Energy Systems Department for assistance in design of the experiment and for providing the test samples, to J. P. Rudd for installing the instrumentation on the samples, and to J. S. Goddard and L. R. Layman for programming the data acquisition system and preparing the data reduction software.

REFERENCES

1. E. H. Christianson, "Large Coil Program Conductor LHe Heat Transfer and Heater Verification Test Analysis," General Dynamics Report No. GDC 91Z0122 (1980); E. H. Christianson and S. D. Peck, "Pool Boiling LHe Heat Transfer in Vertical Conductor Packs," paper JB-2 of these proceedings.
2. S. Shimamoto, T. Ando, H. Hijama, H. Tsuji, K. Yoshida, E. Tada, M. Nishi, K. Okuno, K. Koizumi, K. Oka, and K. Yasukochi, "Japanese Design of a Test Coil for the Large Coil Task," paper presented at the 8th Symposium on Engineering Problems of Fusion Research, November 1979; M. Nishi, private communication.
3. P. F. Michaelson, R. Quay, R. F. Koenig, P. L. Walstrom, and J. S. Goddard, "Heat Transfer and Helium Replenishment in Cabled Conductor Cooling Channels," in Advances in Cryogenic Engineering, Vol. 25, p. 398.
4. C. L. Linkenhoker, private communication.

Table I. Comparison of Steady-State Cryostability Parameters for the Pool-Boiling LCT Coils

Coil	I_{op} (kA)	Unit cell dims. (cm)	j_{av} over unit cell (kA/cm^2)	Wetted perimeter (cm)	Cu cross section (cm^2)	Cu resistivity at field (Ω-cm)	Meas. min heat flux (W/cm^2)	Ohmic heating flux (W/cm^2)	Meas. min power/unit cell vol. (W/cm^3)	Ohmic heating power/unit vol. (W/cm^3)
GE	10.9	1.06 high 4.38 wide	2.4	13.8	3.0	5.5×10^{-8} at 7.5 T	0.13 at 0°	0.14	0.38 at 0°	0.42
GD	10.3	3.42 high 1.15 wide	2.6	12.0[a]	2.4	4.0×10^{-8} at 6.8 T	0.17 at 90°	0.15	0.52 at 90°	0.45
Japan	10.2	2.73 high 1.55 wide	2.4	5.4[b]	2.3	5.1×10^{-8} at 8 T	0.86 at 90°	0.42	1.09 at 90°	0.55
LCS		1.30 high 3.20 wide		10.0			0.18 at 0°		0.40 at 0°	

[a] Includes area of fins.

[b] Derived from projected area of developed surface.

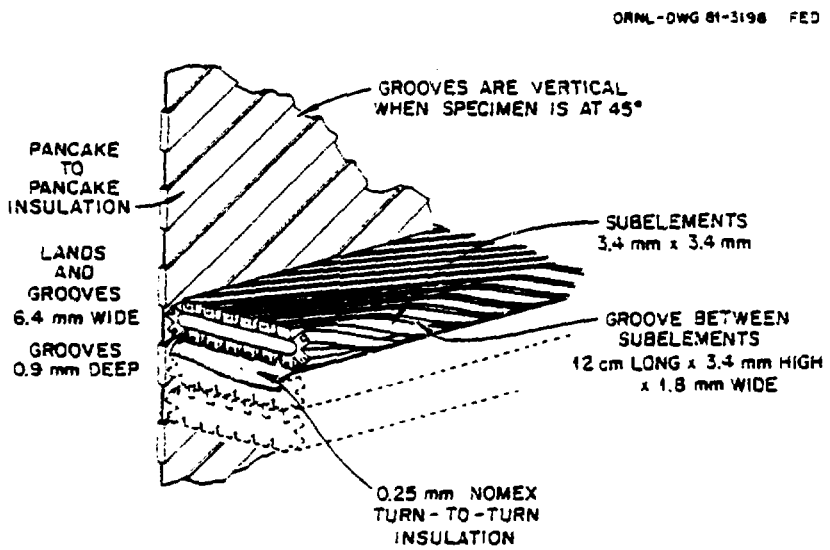
ORNL-DWG 81-3198 FED
GROOVES ARE VERTICAL WHEN SPECIMEN IS AT 45°
PANCAKE TO PANCAKE INSULATION
LANDS AND GROOVES 6.4 mm WIDE
GROOVES 0.9 mm DEEP
SUBELEMENTS 3.4 mm x 3.4 mm
GROOVE BETWEEN SUBELEMENTS 12 cm LONG x 3.4 mm HIGH x 1.8 mm WIDE
0.25 mm NOMEX TURN-TO-TURN INSULATION

Fig. 1

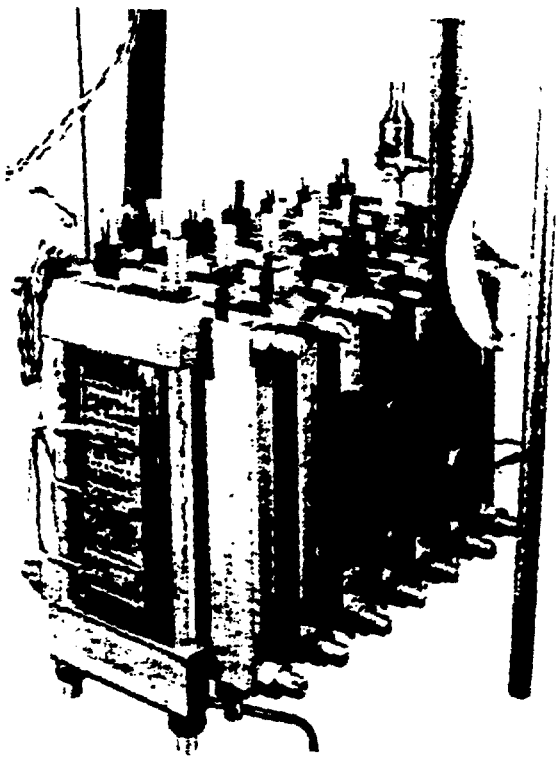

Fig. 2

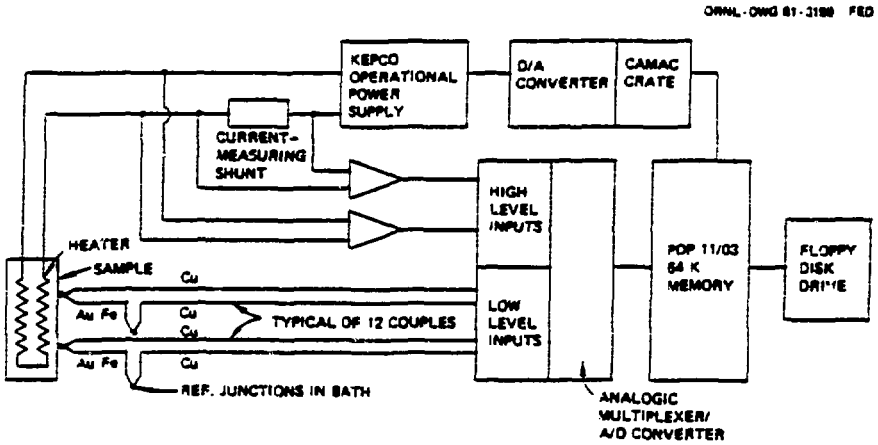
ORNL-DWG 81-3198 FED
KEPCO OPERATIONAL POWER SUPPLY
D/A CONVERTER
CAMAC CRATE
CURRENT-MEASURING SHUNT
HIGH LEVEL INPUTS
LOW LEVEL INPUTS
PDP 11/03 64 K MEMORY
FLOPPY DISK DRIVE
HEATER
SAMPLE
Cu
Au Fe
Cu
Cu
TYPICAL OF 12 COUPLES
Au Fe
Cu
REF. JUNCTIONS IN BATH
ANALOGIC MULTIPLEXER/ A/D CONVERTER

Fig. 3

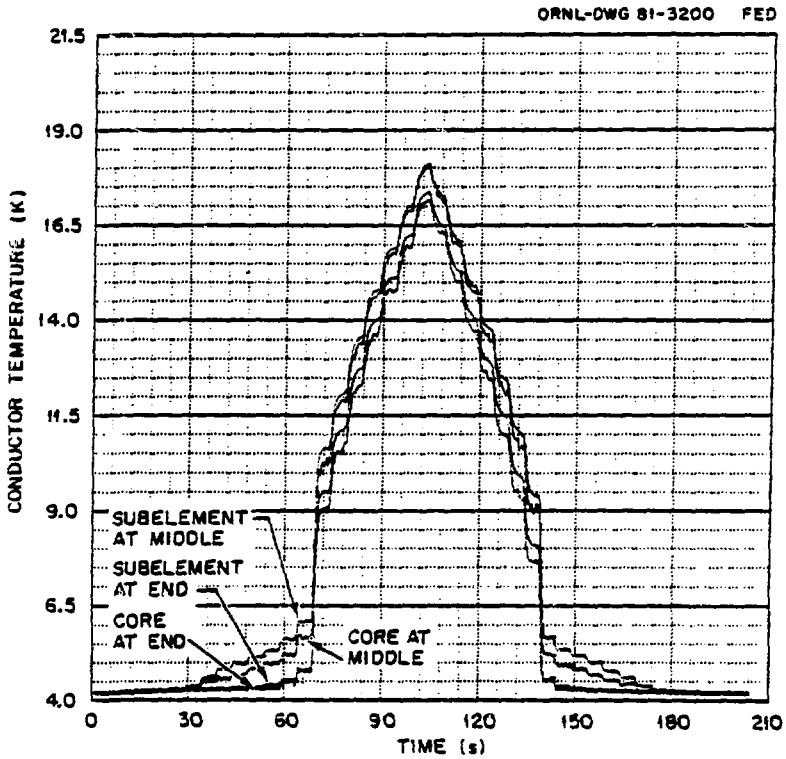
ORNL-DWG 81-3200 FED
CONDUCTOR TEMPERATURE (K)
21.5
19.0
16.5
14.0
11.5
9.0
6.5
4.0
0
30
60
90
120
150
180
210
TIME (s)
SUBELEMENT AT MIDDLE
SUBELEMENT AT END
CORE AT END
CORE AT MIDDLE

Fig. 4

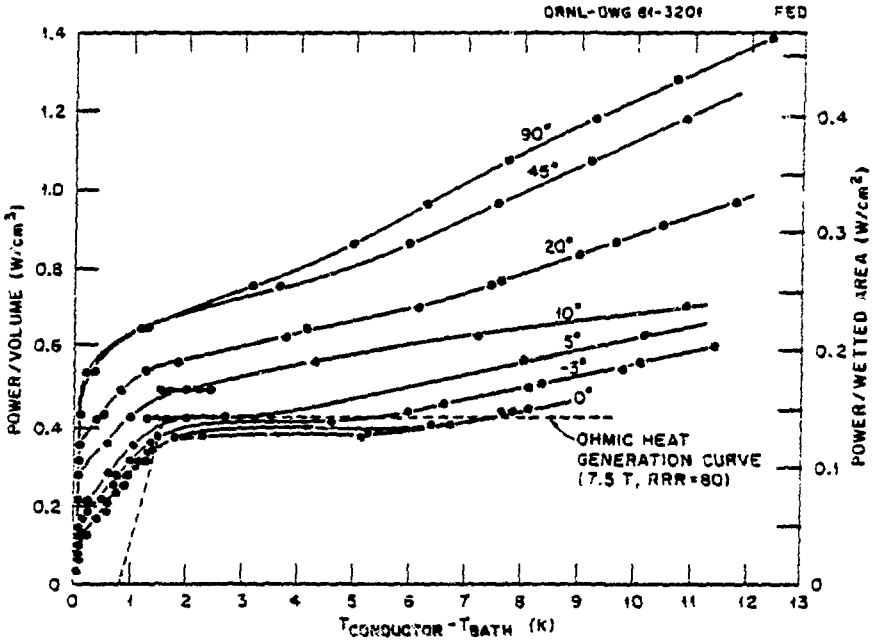
ORNL-DWG 84-3201 FED
POWER/VOLUME (W/cm³)
POWER/WETTED AREA (W/cm²)
T CONDUCTOR - T BATH (K)
90°
45°
20°
10°
5°
-3°
0°
OHMIC HEAT
GENERATION CURVE
(7.5 T, RRR=80)

Fig. 5

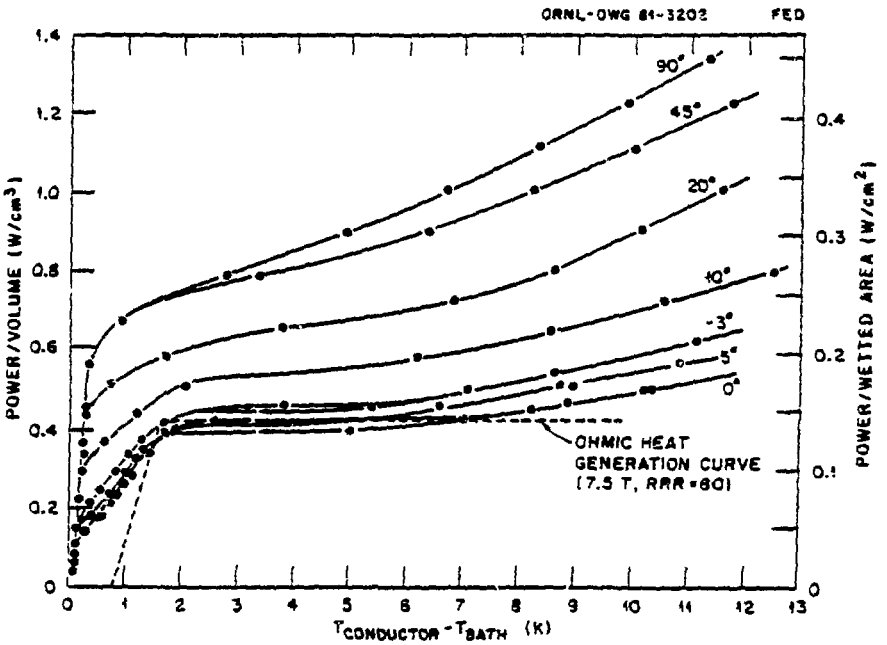
ORNL-DWG 81-3202 FED
POWER/VOLUME (W/cm³)
POWER/WETTED AREA (W/cm²)
T CONDUCTOR - T BATH (K)
90°
45°
20°
10°
-3°
5°
0°
OHMIC HEAT
GENERATION CURVE
(7.5 T, RRR=80)

Fig. 6

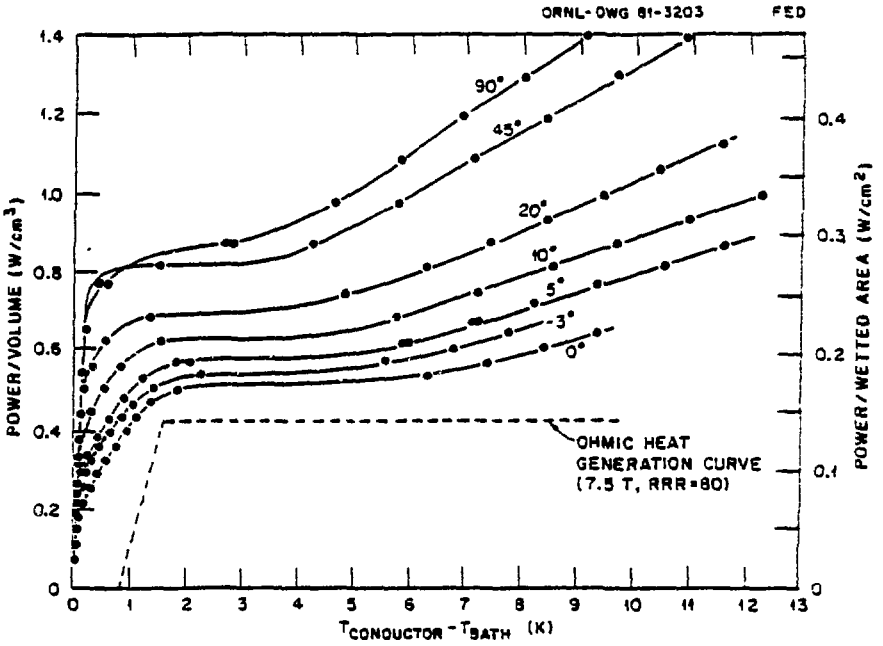
ORNL-DWG 81-3203 FED
POWER/VOLUME (W/cm³)
POWER/WETTED AREA (W/cm²)
T CONDUCTOR - T BATH (K)
90°
45°
20°
10°
5°
-3°
0°
OHMIC HEAT
GENERATION CURVE
(7.5 T, RRR=80)

Fig. 7

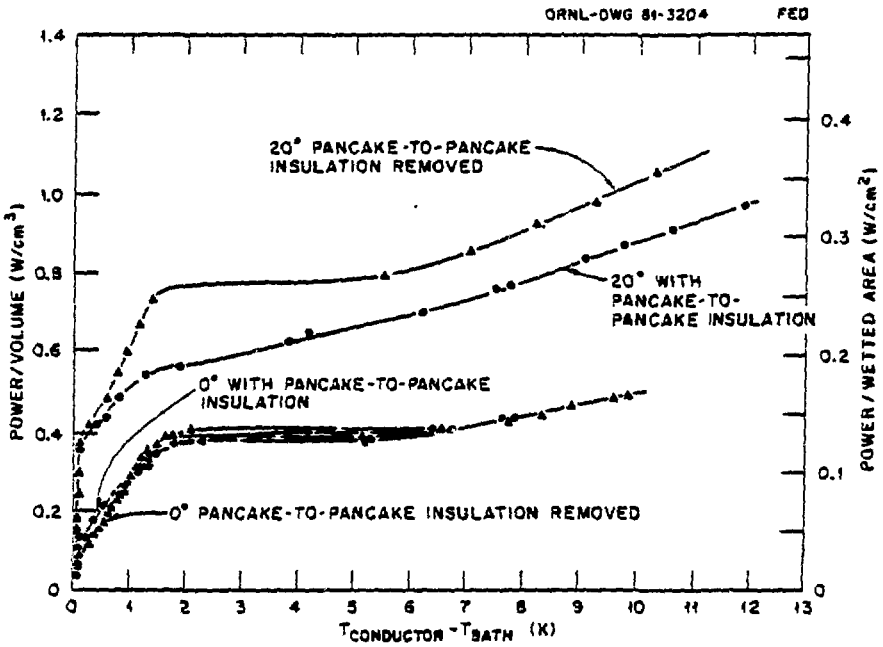
ORNL-DWG 81-3204 FED
20° PANCAKE-TO-PANCAKE INSULATION REMOVED
20° WITH PANCAKE-TO-PANCAKE INSULATION
0° WITH PANCAKE-TO-PANCAKE INSULATION
0° PANCAKE-TO-PANCAKE INSULATION REMOVED
POWER/VOLUME (W/cm³)
POWER/WETTED AREA (W/cm²)
T CONDUCTOR - T BATH (K)
0
0.2
0.4
0.6
0.8
1.0
1.2
1.4
0.1
0.3
0
1
2
3
4
5
6
7
8
9
10
11
12
13

Fig. 8